

STUDIES OF TRANSVERSE SINGLE-PASS BEAM BREAKUP IN E-LINAC

Dobrin Kaltchev, Richard Baartman, Yu-Chiu Chao, Philipp Kolb, Shane Koscielniak, Lia Merminga, Amiya Mitra, Vladimir Zvyagintsev

Abstract

This paper describes time-domain simulations of single-pass transverse beam-breakup (BBU) effects in the TRIUMF/ARIEL E-linac. Using dipole-HOM parameters for the 9-cell cavity obtained with CST Microwave Studio, we evaluate the r.m.s. bunch orbit offsets at linac exit as a function of the average beam current. This allows to evaluate the effectiveness of the HOM absorbers for two different modes of machine operation.

INTRODUCTION

This paper presents the results from our simulations of single-pass transverse beam-breakup (BBU) effects in the electron linear accelerator, E-linac, which is the centre piece of the ARIEL[1] facility under construction at TRIUMF. For the initial operation of E-linac, a 300 KeV electron beam will be injected into a 9-cell cavity (operated at gradient 10 MV/m) followed by a beam transport line – quadrupoles and a magnetic dipole chicane, and then accelerated in the main linac section consisting of four such cavities to a final energy of 50 MeV. At the time of writing, a 1.3 GHz 9-cell modified TESLA-style cavity, but with asymmetric end cells and beamline absorbers rather than hook couplers, is proposed. The layout and lattice are shown on Figure 1. The multi-bunch BBU is expected to cause amplification of the trajectory jitter, which translates into an equivalent growth of the phase-space area swept out by the beam (i.e. effective emittance). Because every bunch feels the accumulated effects of the long-range wakefields of all the preceding bunches, the amplitude of oscillation of the bunches increases as the bunch train travels down the linac. The conditions for this orbit growth to occur are injection errors or cavity misalignments, combined with the presence of dipole high-order modes (HOMs) in the cavity field with high quality factors Q and shunt impedances R_d . In particular, a D3 TE-like dipole HOM with frequency around 2.58 GHz and a high Q ($> 10^5$) is known to exist – TESLA design report [2]), and it has also been found in the present study with CST.

The paper describes our procedure for evaluating the effectiveness of the HOM absorbers. The BBU effect is damped by the random HOM detuning provided by cavity manufacturing errors, but enhanced by bunch-to-bunch charge fluctuations [3]. We assume pessimistic values for both these quantities: small detuning 0.1 MHz, and large (5%) bunch-charge fluctuations.

A special feature of E-linac with regard to BBU is the continuous (cw) beam with bunch repetition rate either

650 MHz (fission beam) or 100-110 MHz (high-brightness beam) for the same average current (10 mA). We study both modes of operation and show that the high brightness regime is more affected by the BBU.

E-LINAC OPTICS AND BBU TOOL

The BBU tool must model correctly both the acceleration and transverse focusing. Further, because of the strong HOM deflection at low-energy injection, it was found important for the first 9-cell cavity that the HOM kick describing the long-range wake field effect may be applied at an arbitrary longitudinal location inside the cavity.

We have adapted the basic block of TALOBBU [5], originally designed for beamlines composed of thin cavities and quadrupoles, to work in a (matrix – HOM-kick – matrix) scheme, where the matrix represents the lumped focusing action of all optics elements to and after the kick, including the rf focusing. The HOM kick is taken in its relativistic approximation [4], [5]. It combines the action of all modes present in the cavity and, being inversely proportional to the beam momentum, is strongest for the first cavity. There we have chosen to apply the kick at the midpoint where $\beta = 0.987$, considered sufficiently relativistic.

An optics code that includes standing-wave accelerating structures as optics elements was created by inserting the 9-cell cavity matrix in MadX. The matrix is derived by integrating numerically the equations of motion in a standing-wave structure [6] (see Appendix). The procedure is preceded by an ASTRA run [7], which serves to optimize the cavity phases and also provides bench-marking for bend-free lattice sections.

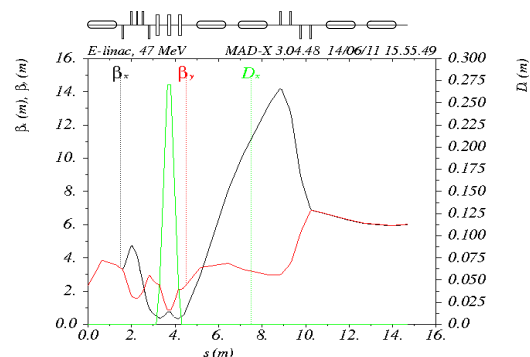


Figure 1: E-linac lattice used in BBU simulations

BBU MODEL

Assume that, due to injection errors and/or misalignment, the beam is off-centered in the cavities. The dipole HOMs in such case cause individual-bunch orbit offsets with respect to the average orbit. When combined with corresponding orbit angle variations, these translate into effective emittance dilution. The r.m.s value of these offsets computed over a long tracking pulse are required to be only a small fraction of the unperturbed beam size. Our goal here is to estimate this fraction.

In the simulations, we assume an injection error at the first cavity entrance $x_0=1$ mm equal to one-third of the r.m.s. beam size. A zero-emittance beam, aligned to the beam ellipse at this point, is tracked in the presence of the 26 dipole HOMs described in the next section. The beam consists of 10^6 bunches, equally spaced, i.e. a tracking pulse duration 1.4, or 10 msec, depending on the mode of operation. The cavity-to-cavity HOM frequency spread is assumed to be random Gaussian distributed with r.m.s. value $\sigma_{\Delta f} = 0.1$ MHz. A bunch-to-bunch charge jitter is also imposed with an r.m.s value 5% of the nominal bunch charge q ($\sigma_{\Delta q}/q = 0.05$). In absence of HOM excitations, the beam exits at a distance $x_{out}=0.14$ mm from the chamber axis. With HOMs, and for a fixed random seed, the exit coordinate x_{out}^{HOM} varies over the entire bunch train as it performs a coherent betatron oscillation. It can be shown, [4], that under the HOM action only, and assuming stable conditions with regard to BBU, the beam centroid tends to a steady state, whose value we denote with $x_{out}^{s.s.}$. An r.m.s. bunch-orbit offset (deflection factor) may be defined as the r.m.s. over the pulse of $|x_{out}^{HOM} - x_{out}^{s.s.}|/x_{out}$. In practice $x_{out}^{s.s.}$ is found approximately as the average of x_{out}^{HOM} over the last 10% of the pulse. In E-linac, the steady state deflections are small; thus $x_{out}^{s.s.} \approx x_{out}$.

DIPOLE HOMS

For a cavity loaded with fundamental mode power input couplers, the parameters of 70 HOMs have been computed with Microwave Studio [9] for two cases: with and without HOM absorbers. A set of 26 modes (those for which $R/Q > 0.01$ ohm and $Q_L > 10^4$) are used in the BBU simulations. Their R/Q values depending on mode frequency are shown in Figure 2. For the modes with largest R/Q (> 0.1), the quality factors Q_L are shown in Table 1. It is clear from this table, that for the case with HOM absorbers the BBU effects will be smaller.

Further, most of the BBU effect is due to modes whose frequency is close to machine lines, i.e. integer multiples of the bunch repetition frequency. Figure 2 shows the R/Q values (blue) on both the 650 MHz mesh (red) and the mode dense 100 MHz mesh (green). The figure suggests that the high-brightness beam will be more affected by HOM.

05 Beam Dynamics and Electromagnetic Fields

D05 Instabilities - Processes, Impedances, Countermeasures

Table 1: Dipole HOM parameters for modes that satisfy the condition ($Rd/Q > 0.1$ ohm and $Q_L > 10^5$). A larger set (26 modes) is used in BBU tracking.

f, GHz	R/Q, Ω	$Q_L^{w/o \text{ absorber}}$	Q_L^{absorber}
1.878	0.133	189000.	189000.
1.881	1.03	522000.	521000.
2.326	0.738	5.92×10^9	12800.
2.558	14.1	187000.	76300.
2.562	64.2	1.91×10^6	114000.
3.016	0.614	576000.	287000.
3.065	0.191	6.78×10^8	3.38×10^7
3.069	0.741	139000.	138000.

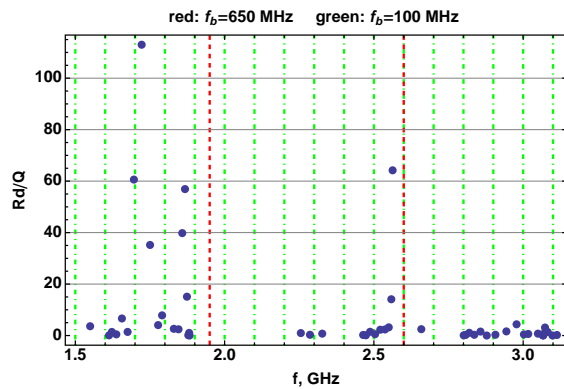


Figure 2: The 26 R/Q values shown on both the 650-MHz mesh (red) and the more dense 100-MHz mesh (green). The blue points have a larger chance to fall in the vicinity of a green line than red.

RESULTS

Sample Pulse Shape

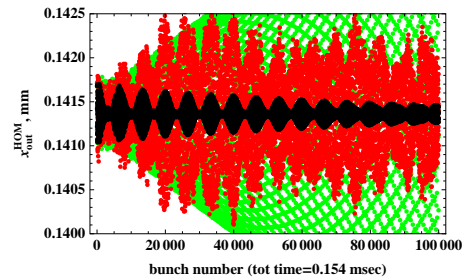


Figure 3: Sample tracking-pulse shape at linac exit: $\sigma_{\Delta f} = \sigma_{\Delta q} = 0$ (green); $\sigma_{\Delta f} = 0.1$ MHz and $\sigma_{\Delta q} = 0$ (black); $\sigma_{\Delta f} = 0.1$ and $\sigma_{\Delta q}/q = 5\%$ (red).

The orbit pattern at exit for a single random seed is shown on Figure (fission regime, a cavity without absorbers, the first 10^5 bunches). Without any spreads, i.e. HOM action only, there is a resonant growth (green). A mode frequency spread of 0.1 MHz provides sufficient random detuning to reduce the growth (black), however the pulse partially recovers over a certain period. When both

frequency spread 0.1 MHz and charge jitter of 5% are applied, random oscillations are seen, with nearly constant amplitude over the whole pulse (red).

Rms'Dunch'Orbit'Offsets

Figure 4 shows the rms orbit growth calculated from 20 random machines (10 frequency seeds combined with 10 seeds of random charge jitter): average (top) and maximum (bottom). The corresponding steady state shift is always below 1% (not shown). The high-brightness beam is more affected by BBU, which is explained by the higher bunch charge (factor 6.5), and hence stronger HOM kick, and the larger chance for a HOM to get near a machine line (Figure 2). Including randomly misaligned cavities of 0.5 mm rms did not change this result. For the worst case of random machine, at the top current 30 mA, and without HOM absorbers the beam emittance may double. However, the emittance dilution is negligible for cavity with absorbers for both fission and high-brightness. Even with the very pessimistic assumptions for the stability of the source, the initial E-linac operation at 10 mA is practically not affected: the emittance dilution is well below the diagnostic resolution of 5%.

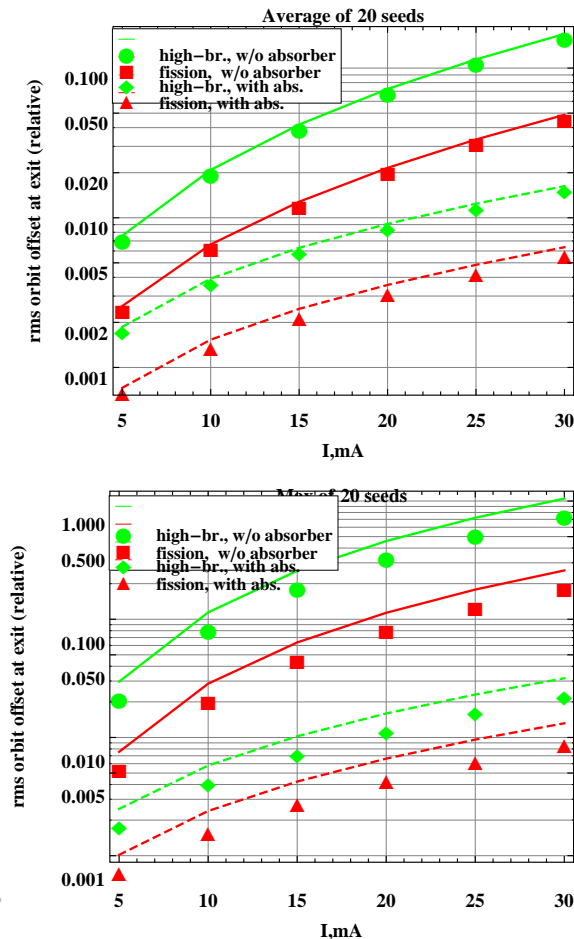


Figure 4: Average (top) and maximum (middle) rms bunch orbit offsets depending on the average current for 20 random machines.

APPENDIX

We follow [6] to integrate numerically the equations of motion (EOM) with longitudinal coordinate z' as the independent variable. In what follows, prime denotes conventional, non-normalized variables: coordinates z' and r' , velocity v' , energy E' and time t' . Introduce normalized quantities: $z = \frac{z'}{\lambda}$, $v = \frac{v'}{c}$, $\gamma = \frac{E'}{mc^2}$, $t = \frac{ct'}{\lambda}$, $r = \frac{r'}{\lambda}$ and $s = \frac{v'}{c}$ = transverse velocity/c (dot means d/dt'). Here $\lambda = c/f$, $f = 1.3$ GHz and c is the speed of light. Given a z - E_z table for the longitudinal electric field E_z at the symmetry axis, we compute ten Fourier coefficients A_m ($m = 1, 3, \dots, 19$). The (normalized) rotationally symmetric field of the standing wave is then represented as:

$$\begin{aligned} E_z &= \sum_m^N A_m I_0(k_m r') \cos \Psi \\ E_r &= \sum_m^N A_m \frac{m\pi}{k_m L'} I_1(k_m r') \sin \Psi \\ B_\theta &= \sum_m^N A_m \frac{2\pi}{k_m \lambda} I_1(k_m r') \cos \Psi \\ \Psi &= \frac{m\pi}{L'} (z' - \frac{L'}{2}); \quad k_m = \sqrt{(m\pi/L')^2 - (2\pi/\lambda)^2}. \end{aligned}$$

Here L' is the cavity length. For a particle with zero azimuthal velocity component, the EOM are:

$$\begin{aligned} \frac{d\gamma}{dz} &= \frac{dE_z}{dz}, \quad \frac{dt}{dz} = \frac{1}{v}, \quad \frac{dr}{dz} = \frac{s}{v}, \quad \frac{ds}{dz} = \\ &= -\frac{s}{\gamma} \frac{dE_z}{dz} - \frac{\alpha}{v\gamma} (E_r \sin[2\pi t + \phi_0] - v B_\theta \cos[2\pi t + \phi_0]), \\ \frac{dE_z}{dz} &\equiv -\alpha (E_z \sin[2\pi t + \phi_0] + s B_\theta \cos[2\pi t + \phi_0]), \end{aligned}$$

where $\alpha \equiv \frac{\lambda E_0}{mc^2}$ and $E_0 = 10, 20$ MV/m. These equations have been solved and single-particle trajectories compared with Astra for the same E_z table and initial phase ϕ_0 . The agreement is excellent for relativistic particles, while for the first cavity some small deviations (several %) have been observed.

REFERENCES

- [1] L. Merminga, *et al*, ARIEL: TRIUMF's Advanced Rare Isotope Laboratory, these proceedings.
- [2] TESLA Technical Design Report, Part 2: The Accelerator, Chap.3, Table 3.2.2, DESY, March 2001.
- [3] J. Tückmantel, PRST Accel. Beams 13, 011001 (2010)
- [4] R.L. Gluckstern, R.K. Cooper and P.J. Channell, *Cumulative Beam Breakup in RF Linacs*, Part Acc, vol 16 pp 125-153.
- [5] D. Jeon, L. Merminga, *et al*, NIM A 495 (2002) 85-94.
- [6] E.E. Chambers, *Particle Motion in a Standing Wave Linear Accelerator*, SLAC report 1967
- [7] Klaus Flöttmann, ASTRA, <http://www.desy.de/~mpyf10>
- [8] M. Schuh, J. Tückmantel, J.L. Biarrotte, D. Kaltchev, *Code Benchmarking of Higher Order Modes Simulation Codes*, CERN-sLHC-Project-Note-0010, CERN, 2010.
- [9] CST, www.cst.com